Available online at www.sciencedirect.com
ScienceDirect
Surface & Coatings Technology 201 (2007) 9141–9145
SURFACE & COATINGS TECHNOLOGY
www.elsevier.com/locate/surfcoat

Thin film sulphides and oxides of 3d metals prepared from complex precursors by CVD

V.G. Bessergenev [a,*], R.J.F. Pereira [a], A.M. Botelho do Rego [b]

[a] *Universidade do Algarve, FCT, Campus de Gambelas, 8005-139 Faro, Portugal*
[b] *Instituto Superior Técnico, 1049-001 Lisboa, Portugal*

Available online 13 May 2007

Abstract

Iron, cobalt and manganese sulphide thin films have been prepared by CVD using $Fe[(C_2H_5)_2NCS_2]_3$, $Co[(C_2H_5)_2NCS_2]_3$ and MnPhen $[(C_2H_5)_2NCS_2]_2$ complex compounds (CCs) as precursors. The respective oxides were prepared by annealing the sulphide thin films in the presence of oxygen (Fe_3O_4, Fe_2O_3, Co_3O_4 and γ-Mn_3O_4) or by CVD from the same precursor in Ar/O_2 atmosphere (Fe_3O_4, Fe_2O_3). Thin film structure was investigated by high-resolution Grazing-Incidence X-ray Diffraction (GIXRD) at the DESY/HASYLAB (Hamburg, Germany). Chemical composition of thin films was studied by high-resolution Laser Ionization Mass Spectrometry (LIMS) technique. Magnetic structure of iron oxides and sulphides was characterized by Conversion Electron Mössbauer Spectroscopy (CEMS).

PACS: 61.72.Vv; 81.05.Hd; 81.15.Gh
Keywords: Thin films; CVD; Iron; Cobalt and manganese sulphides

1. Introduction

Thin film oxides and sulphides of 3d metals are of actual interest from both the fundamental and technological points of view, given their use as catalytic [1], photovoltaic [2] and magnetic layers [3]. In particular, iron pyrite (FeS_2) and magnetite (Fe_3O_4) have attracted great interest, the first due to their possible applications as absorber materials in thin film solar cells and the second as ferromagnetic oxides for room temperature spin injection for spintronic devices. It has been observed [2, 3] that electronic and magnetic properties of iron sulphides and oxides critically depend on the stoichiometry and crystallographic quality of the thin films. The dependency is explained by the existence of various crystal modifications of iron sulphides and iron oxides with their composition varying between FeS and FeS_2, and FeO and Fe_2O_3 respectively. Development of the appropriate precursors for the deposition of the doped iron sulphide and oxide thin films with p- and n-type of conductivity is also of great interest. This can be achieved by doping iron sulphide (oxide) with Mn and Co.

Our present objectives were, firstly, to verify whether the dithiocarbamate complexes of Fe, Co and Mn can be used as precursors for CVD of sulphide and oxide films. Next, we investigated whether the Fe–S bonds existing in complexes $Fe[(C_2H_5)_2NCS_2]_3$ would facilitate formation of the pyrite films. Finally, we studied the oxidation stability of sulphide films in view of transforming sulphides into a variety of oxides *in-situ* during the CVD process, by mixing oxygen with the CCs vapours.

In this work, FeS_{2-x}, CoS_{2-x}, MnS, Fe_3O_4, Fe_2O_3, Co_3O_4 and γ-Mn_3O_4 thin films were prepared by CVD. The effects of deposition conditions on chemical composition and crystal structure of the films were studied.

2. Experimental details

Iron, cobalt and manganese sulphides were obtained from a series of metal dithiocarbamates as precursors, including Tris (DiethylDitiocarbamato)Iron(III) (FeL_3), Tris(DiethylDitiocarbamato)Cobalt(III) (CoL_3) and $MnPhenL_2$, with $L=(C_2H_5)_2NCS_2$,

* Corresponding author. Postal address: Algarve University, FCT, Campus de Gambelas, 8005-139 Faro, Portugal. Tel.: +351 289 800 900x7613; fax: +351 289 800 066.
E-mail address: vbess@ualg.pt (V.G. Bessergenev).

0257-8972/$ - see front matter © 2007 Elsevier B.V. All rights reserved.
doi:10.1016/j.surfcoat.2007.05.017

and Phen = 1,10-phenanthroline. Thin films were synthesised in vacuum with the exception of FeS_{2-x}, where Di-tert-butyldisulphide, $[(CH_3)_3C]_2S_2$ (TBDS) vapours were used to increase sulphur content. The respective oxides were obtained from the same precursors by adding Ar/O_2 mixture into the reactor. Thermal properties of all the precursors used are very similar, therefore the synthetic procedures will be explicitly described for FeS_{2-x} only.

The apparatus used for low-pressure CVD has been described in detail elsewhere [4,5]. Briefly, FeS_{2-x} films were obtained in a standard vacuum apparatus with a turbo-molecular pump (ALCATEL TMP 5400 CP) creating vacuum down to $\sim 5\times10^{-7}$ mbar. Precursors were vapourized from an open-surface evaporator. The temperature of the evaporator was set in the 180–270 °C range and that of the substrate in the 340–550 °C range. The pressure of volatile decomposition products of the precursor achieved 10^{-4}–10^{-1} mbar depending on the parameters of the process. The temperature of the TBDS evaporator was set in the 200–226 °C range in order to increase the vapour pressure of TBDS. The TBDS vapours were supplied into the reactor by the continuous flux of argon.

The mass of the precursor ranged from 0.065 to 2.000 g, resulting in the thin film thickness in the 30–1100 nm range. The typical growth rates were between 7 and 62 nm/min. Glass and fused-silica substrates were used, with the typical deposition conditions presented in Table 1. Note that no films were formed at the substrate temperatures ($T_{substrate}$) below 320 °C.

Crystal structure of as-prepared thin films was analysed by high-resolution Grazing-Incidence X-ray Diffraction (GIXRD) and regular θ–2θ scans at the DESY/HASYLAB synchrotron radiation laboratory. Grazing-incidence angles α_i varied between 0.9 and 1.0°. Synchrotron radiation wavelength was equal to $\lambda = 0.11315$ nm.

Trace analysis of the FeS_{2-x} films was performed by Laser Ionization Mass Spectrometry (LIMS) using double-focusing mass spectrometer with Mattauch–Herzog geometry and laser plasma ion source (EMAL-2). Energy output of Nd-YAG laser (wavelength of 1064 nm), pulse duration, repetition rate and diameter of laser spot on sample surface were adjusted in order to achieve evaporation and ionization of the deposited films only. The glass substrates are transparent for Nd-YAG laser radiation and practically were not affected by the radiation. The measured concentration of Si, the main component of the substrate, never exceeded 10^{-2} wt.% at the chosen laser power density of *ca.* 1×10^9 W/cm^2. The surface area analyzed was *ca.* 0.5 cm^2. The concentrations of impurities were quantified against Fe as an internal standard.

Conversion Electron Mössbauer Spectra (CEMS) were obtained at room temperature from thin films deposited on

Table 1
Typical conditions for the thin film synthesis

Sample	Precursor	Precursor weight, g	Substrate	Thickness, nm	$T_{substrate}$, °C	$P_{Max.}$, mbar	Flux, % Ar/O_2
FS-1Q	A	0.4653	Quartz	n/d	500	3.2×10^{-4}	–
FS-2Q		0.4586	Quartz	477	450	1.1×10^{-3}	–
FS-5Q		0.2986	Quartz	399	350	2.5×10^{-1}	–
FS-6Q		0.5026	Quartz	247	500	4.5×10^{-1}	–
FS-7Q		0.4991	Quartz	475	450	4.6×10^{-1}	–
FS-11Q		2.0000	Quartz	1122	450	–	–
FS-16Q		0.3202	Quartz	585	340	2.1×10^{-4}	–
FS-18Q		0.4007	Quartz	585	400	4.3×10^{-4}	–
FS-22	A+B	0.3044	Glass	65	450	5.1×10^{-4}	50/0
FS-32		0.2994	Quartz	55	450	2.3×10^{-1}	51.5/0
FS-43		0.3996	Quartz	218	480	1.9×10^{-1}	51.3/0
FS-47		0.3995	Quartz	524	430	7.0×10^{-2}	52/0
FS-49		0.4619	Quartz	557	520	8.1×10^{-2}	51.2/0
FS-51		0.4002	Quartz	371	432	1.3×10^{-1}	52.8/0
FS-53		0.4002	Quartz	371	400	2.3×10^{-1}	52.8/0
FS-54		0.4002	Quartz	382	400	1.6×10^{-1}	52/0
FO-01	A	0.2996	Glass	52	450	6.7×10^{-2}	50/50
FO-02		0.2996	Glass	94	450	6.7×10^{-2}	50/50
FO-04		0.2999	Quartz	125	500	4.3×10^{-2}	50/50
FO-05		0.2998	Glass	166	400	6.7×10^{-2}	50/50
FO-07		0.3005	Glass	106	400	7.0×10^{-2}	50/1
FO-09		0.2997	Glass	137	400	7.3×10^{-2}	50/10
FO-11		0.3002	Glass	190	400	8.0×10^{-2}	50/5
CoS-01	C	0.3350	Quartz	320	400	1.5×10^{-4}	–
CoS-04		0.3049	Quartz	350	350	5.6×10^{-5}	–
CoS-06		0.3590	Quartz	240	500	8.0×10^{-5}	–
MnS-01	D	0.3210	Quartz	380	450	6.2×10^{-5}	–
MnS-04		0.2998	Quartz	370	500	4.3×10^{-5}	–
MnS-06		0.2499	Quartz	330	400	1.7×10^{-4}	–
MnS-08		0.2803	Quartz	250	350	1.1×10^{-4}	–

Precursors: A = $Fe[(C_2H_5)_2NCS_2]_3$, B = $[(CH_3)_3C]_2S_2$ (TBDS), C = $Co[(C_2H_5)_2NCS_2]_3$, D = $MnPhen(Et_2NCS_2)_2$. Atmosphere: 100% corresponds to 25 ml_n/min (ml_n — millilitres at normal atmospheric pressure).

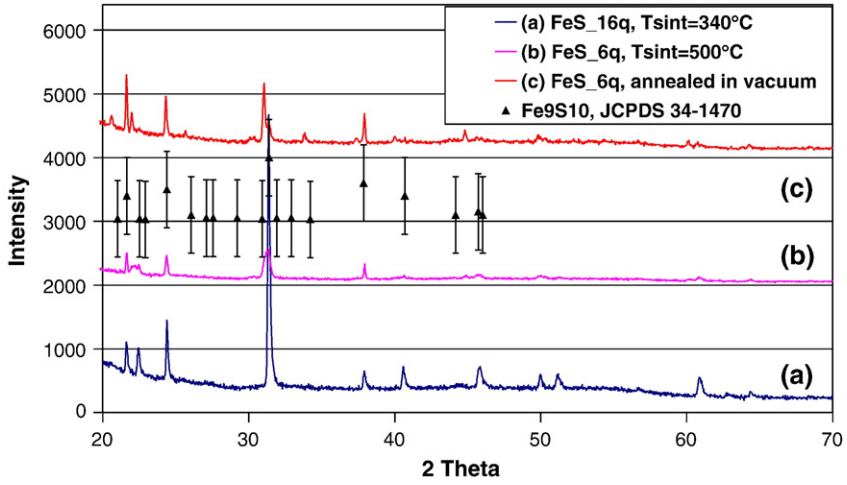

Fig. 1. GIXRD pattern of the as-deposited and vacuum-annealed iron sulphide thin films on fused-silica substrates.

fused quartz substrates, on a Wissel constant acceleration spectrometer, using a Rikon-5 detector and a ^{57}Co/Rh source. The resulting spectra were calibrated with α-Fe foil at room temperature and fitted using an integrated least-squares computer program [6] to determine hyperfine parameters of actual Fe phases.

3. Results and discussion

Different techniques have been used to prepare iron pyrite (FeS_2), including natural pyrite flash evaporation [7], MOCVD with Ironpentacarbonil ($Fe(CO)_5$) and TBDS as precursors [8] and double source (metallic Fe and elemental S) vacuum vapour deposition [9]. The phase diagram for Fe–S system is partly unknown, still, pyrite could be formed using $Fe(CO)_5$ at 5×10^{-3} mbar and TBDS at 2 mbar and *ca.* 575 °C substrate temperature [8], whereas in [9] it was prepared by double source vacuum vapour deposition technique at the S/Fe flux ratio of 6.8 to 14.8 and temperature over 300 °C.

We expected that the existing Fe–S bonds of the FeL_3 precursor would facilitate formation of the pyrite phase in the deposited film. There exist six sulphur atoms for each iron atom in the FeL_3 precursor, more than sufficient to produce pyrite. The results of the XRD studies of the as-prepared and annealed FeS_{2-x} thin films are shown in Fig. 1. We see that the films deposited on fused-silica substrates at 340°C (Table 1, precursor A) have the Fe_9S_{10} crystal structure (JCPDS-ICDD 34-1470). Indeed, it is known that FeS_2 heated in vacuum can easily loose some sulphur, yielding films of the FeS_{2-x} composition. The equilibrium can be shifted towards FeS_2 by using a large excess of TBDS over Fe [8]. Therefore, to increase the sulphur content in the films, a series of experimental runs was made in presence of added TBDS vapours (Table 1, precursor A+B).

Fig. 2 presents some of the Conversion Electron Mössbauer Spectra (CEMS) recorded from the as-deposited FeS_{1+x} thin films synthesised using $Fe[(C_2H_5)_2NCS_2]_3$ and $[(CH_3)_3C]_2S_2$ (TBDS) as precursors. We conclude that the temperature of synthesis and the TBDS vapour pressure essentially influence the phase composition of the thin films. Higher synthesis temperatures lead to losses of sulphur and to the formation of the FeS_{1+x} phases (Troilite-like FeS) with low sulphur content. Increased TBDS vapour pressures lead to higher sulphur content and to the formation of the FeS_{2-x} phases.

Average concentrations of the impurities in the FeS_{2-x} films shown in Table 2 were obtained by LIMS. Large sample-to-sample variations are observed for Ca, Zn and W impurities. We were unable to obtain a representative statistics on the impurities, as only five samples were studied by LIMS, therefore, the presence of some impurities, such as P, Ca, Zn

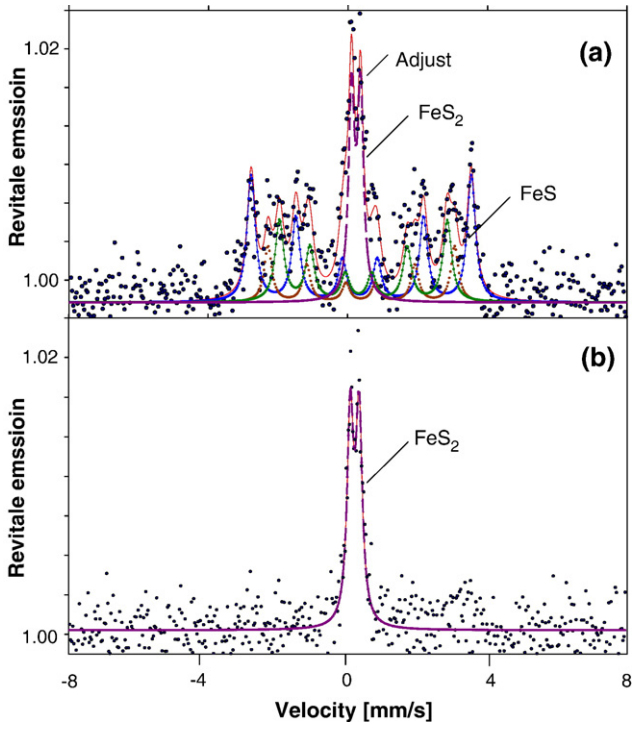

Fig. 2. Room temperature CEMS spectrum of the as-deposited FeS_{1+x} film, sample FS-47 (a) and FS-32 (b).

Table 2
The results of mass-spectral analysis (standard deviation = 0.15 ÷ 0.25), the values are shown in %; n/d — not detected, the detectability threshold is given in brackets

Impurity	FS-1Q	FS-2Q	FS-5Q	FS-6Q	FS-7Q
C	2×10^{-1}	1×10^{-1}	2×10^{-2}	$\leq6\times10^{-3}$	2×10^{-1}
N	3×10^{-2}	1×10^{-2}	$\leq2\times10^{-3}$	$\leq2\times10^{-3}$	1×10^{-2}
Na	2×10^{-1}	1×10^{-2}	2×10^{-3}	2×10^{-2}	3×10^{-2}
Mg	2×10^{-2}	4×10^{-3}	5×10^{-4}	1×10^{-4}	3×10^{-3}
Al[a]	$<1\times10^{-1}$	$<1\times10^{-1}$	$<5\times10^{-2}$	$<5\times10^{-2}$	$<1\times10^{-1}$
P	1×10^{-2}	2×10^{-3}	9×10^{-4}	4×10^{-4}	3×10^{-3}
Cl	2×10^{-2}	8×10^{-3}	6×10^{-3}	2×10^{-2}	4×10^{-2}
K	8×10^{-2}	5×10^{-2}	4×10^{-3}	1×10^{-2}	5×10^{-2}
Ca	2×10^{-1}	5×10^{-2}	4×10^{-2}	3×10^{-3}	1×10^{-1}
Cr	5×10^{-2}	1×10^{-2}	9×10^{-3}	2×10^{-2}	2×10^{-2}
Mn	3×10^{-2}	1×10^{-2}	1×10^{-2}	2×10^{-2}	5×10^{-3}
Co	2×10^{-2}	1×10^{-2}	3×10^{-2}	2×10^{-2}	1×10^{-2}
Ni	1×10^{-2}	4×10^{-2}	5×10^{-2}	7×10^{-2}	4×10^{-2}
Cu	2×10^{-1}	8×10^{-2}	3×10^{-1}	2×10^{-1}	2×10^{-1}
Zn	2×10^{-1}	2×10^{-2}	7×10^{-3}	3×10^{-3}	3×10^{-3}
W	n/d (6×10^{-4})	n/d (6×10^{-4})	n/d (6×10^{-4})	n/d (6×10^{-4})	2×10^{-2}

[a] Detectability limited by the superimposed signal of doubly charged ions of the matrix.

for the FS-1Q and W for FS-7Q remained unclear, being most probably just occasional. Nevertheless, the data of Table 2 provide good quantitative estimates for the typical impurity concentrations in our sulphide films.

The results of GIXRD analysis of CoS_x thin films are presented on Fig. 3. We see that cobalt sulphide thin films are very well crystallised. These films were prepared in the 350–500 °C temperature range, with all samples showing Co_9S_8 crystal structure. The diffraction peak at *ca.* 11° markedly increases at higher temperatures of synthesis, which indicates a reorientation of the micro crystals along a certain preferential axis. However, all of the peaks describing Co_9S_8 (JCPDS 19-364) remain present in the X-ray diffraction patterns at all temperatures tested.

The results of GIXRD analysis of MnS thin films are also shown in Fig. 3. Note that a clear MnS structure (JCPDS 6-518) is formed in the entire temperature range of 350–500 °C, although β-MnS, γ-MnS, or MnS_2 could be alternatively produced.

Iron, cobalt and manganese oxides were prepared using two different procedures. In the first one, previously prepared sulphide thin films were heated in vacuum under low oxygen pressure or in air, in order to study their oxidative stability. Alternatively, iron oxide thin films were prepared using the same precursor $Fe[(C_2H_5)_2NCS_2]_3$, admitting Ar/O_2 mixtures in variable proportions at total pressures of $(4.3\div8)\times10^{-2}$ mbar into the reactor (see Table 1).

The GIXRD results for cobalt and manganese oxides prepared by annealing in air at 1 bar are also shown in Fig. 3. Note that only Co_3O_4 and γ-Mn_3O_4 stoichiometries arise, from an entire set of possible crystal modifications.

CEMS spectra of Fe oxide films were obtained at room temperature. Fig. 4(a) shows magnetite spectra of the as-deposited films prepared at 400 °C in an Ar/O_2 mixture with low oxygen content (50/1 at 7.0×10^{-2} mbar) as an example. The spectrum consists of two sextets, T_d and O_h, which result from the respective tetrahedral A sites (Fe^{3+}) and octahedral B sites (Fe^{2+} and Fe^{3+}) of the inverse spinel crystal cell of magnetite.

The isomer shifts for the A and B sites, of 0.28 and 0.67 mm/s, and their respective hyperfine fields of 49.0 and 45.8 T, are nearly the same as the reported values for ideal magnetite. However, the

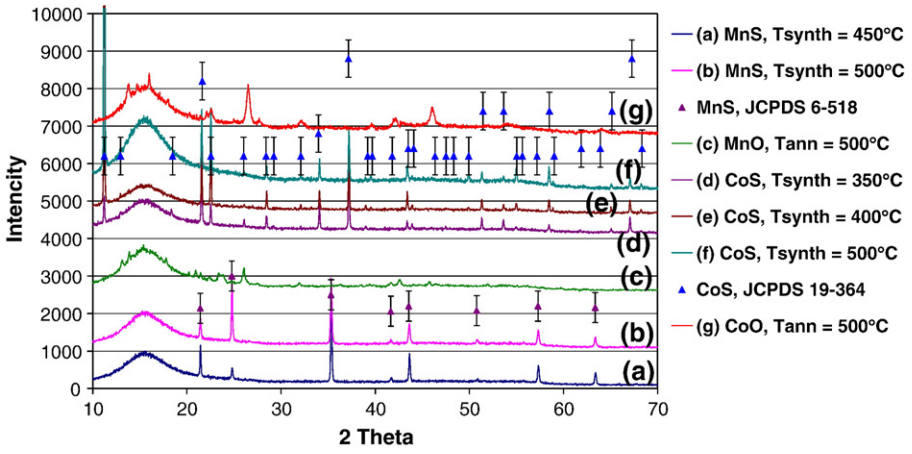

Fig. 3. GIXRD pattern of as-deposited cobalt and manganese sulphide and oxide thin films on fused-silica substrates: a) MnS, T_{synth} = 450°C; b) MnS, T_{synth} = 500 °C; c) γ-Mn_3O_4, T_{ann} = 500 °C; d) CoS, T_{synth} = 350 °C; e) CoS, T_{synth} = 400 °C; f) CoS, T_{synth} = 500 °C; g) Co_3O_4, T_{ann} = 500 °C.

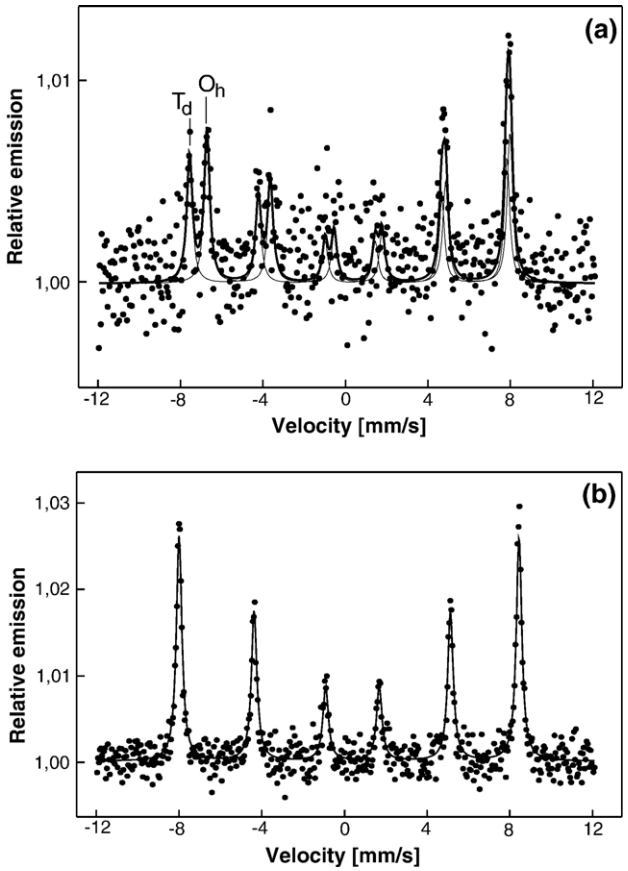

Fig. 4. Room temperature CEMS spectra: (a) magnetite film deposited by CVD at a substrate temperature of 400 °C, in Ar/O_2 atmosphere at 7×10^{-2} mbar with Ar/O_2 is 50/1, (b) stoichiometric hematite films deposited at 450 °C.

area ratio $I(O_h)/I(T_d)=1.22$ is much lower than the ideal ratio of 2.00 for stoichiometric magnetite. Detailed analysis produced the $Fe_{2.93}O_4$ chemical formula for this sample.

The hematite CEMS spectrum shown in Fig. 4(b) is very similar to those reported for stoichiometric Fe_2O_3. The 3:3:1 relative intensity ratio indicates a predominantly in-plane orientation of the magnetic moments in the film. The measured internal fields have values typical for stoichiometric hematite.

CEMS results demonstrated that magnetite films are obtained from iron sulphide thin films annealed in the vacuum chamber for 30 min at 400 °C under 10^{-1} mbar of air. On the other hand, iron oxide thin films annealed in air at 1 bar have a typical hematite structure.

4. Conclusions

We demonstrated that $Fe[(C_2H_5)_2NCS_2]_3$ and $[(CH_3)_3C]_2S_2$ complex compounds can be used as precursors to prepare a large variety of FeS_{1+x} ($0<x<1$) thin films by CVD synthesis. Similarly, $Co[(C_2H_5)_2NCS_2]_3$ and $MnPhen(Et_2NCS_2)_2$ complex compounds can be used to prepare the respective Co_9S_8 and MnS thin films. Thermal properties of all these complex precursors and the synthesis conditions are very similar, therefore they are especially suitable for synthesis of p- and n-doped iron sulphide thin films.

We found that even during the synthesis the FeS_{1+x} thin films can be easily converted in the presence of Ar/O_2 atmosphere into various iron oxide (FeO_{1+x}) thin films. Cobalt and manganese oxides can be synthesised in the same way.

Our results also permit to produce some recommendations for the production of future solar cells using pyrite thin films. In particular, these films must be suitably protected from heating in air or in presence of water vapours, due to their low oxidative stability. We additionally conclude that a very flexible and versatile multilayer deposition technology can be created, based on CVD with the presently studied complex precursors.

Acknowledgements

The authors are grateful to *Fundação para a Ciência e Tecnologia*, Portugal, for the financial support in the framework of the projects POCTI/43520/FIS/2000, 423/DAAD-ICCTI and project II-01-64 (HASYLAB). This work was also supported by the European Community-Research Infrastructure Action under the FP6 "Structuring the European Research Area" Programme in the framework of IHP-Contract HPRI-CT-1999-00040/2001-00140.

References

[1] W. Weiss, W. Ranke, Prog. Surf. Sci. 70 (2002) 1.
[2] P.P. Altermatt, T. Kiesewetter, K. Ellmer, H. Tributsch, Sol. Energy Mater. Sol. Cells. 71 (2002) 181.
[3] Y. Tokura, Y. Tomioka, J. Magn. Magn. Mater. 200 (1999) 1.
[4] V.G. Bessergenev, I.V. Khmelinskii, R.J.F. Pereira, V.V. Krisuk, A.E. Turgambaeva, I.K. Igumenov, Vacuum 64 (2002) 275.
[5] V.G. Bessergenev, R.J.F. Pereira, M.C. Mateus, I.V. Khmelinskii, E. Burkel, R.C. Nicula, Int. J. Photoenergy 5 (2003) 99.
[6] M.M.P. Azevedo, M.S. Rogalski, J.B. Sousa, Meas. Sci. Technol. 8 (1997) 941.
[7] C. De Las Heras, C. Sanchez, Thin Solid Films 199 (1999) 259.
[8] C. Höpfner, K. Ellmer, A. Ennaoui, C. Pettenkofer, S. Fiechter, H. Tributsch, J. Cryst. Growth 151 (1995) 325.
[9] Y. Sasaki, A. Sugii, K. Ishii, J. Mater. Sci. Lett. 18 (1999) 1193.